Electronic Supplementary Material

Surface-Enhanced Raman Spectroscopy for Size-Resolved Microplastic Detection in Real-world Samples Using Thiophenol Labeling

Jayasree Kumar[a], Arunima Jinachandran[a], Mounika Renduchintala[a], Venugopal Rao Soma[b,c], Vijayakumar Shanmugam[d], Shaik Imamvali[e], Sreenivasulu Tupakula[e], and Rajapandiyan Panneerselvam*[a]

1 *Raman Research Laboratory (RARE Lab), Department of Chemistry, SRM University-AP, Andhra Pradesh, Amaravati, 522240, India*
2 *Advanced Centre of Research in High Energy Materials (ACRHEM), DRDO Industry Academia – Centre of Excellence (DIA-COE), University of Hyderabad, India*
3 *School of Physics, University of Hyderabad, Hyderabad, 500046, India*
4 *Institute of Nano Science and Technology, Mohali, India*
5 *Department of Electronics and Communication Engineering, SRM University-AP Andhra Pradesh, 522240, India*

Corresponding author

E-mail address: rajapandiyan.p@srmap.edu.in (Rajapandiyan Panneerselvam)

Table of contents

equal ratio incubated on an AgNPs@Filter paper substrate were analyzed using 1 mM thiophenol, (b) corresponding linear plot at 1066 cm^{-1}.

Table S2.

Water quality assessment (DI water, saltwater, and lake water).

Figure S8.

(a) SERS spectra of 0.09 mg/mL PS microplastics (250 μm and 2.1 mm) spiked in lake water and salt samples, incubated on an AgNPs@Filter paper substrate, and analyzed using 1 mM thiophenol, (b) corresponding bar graph at 1066 cm^{-1}.

Figure S9.

Bar diagram illustrating the selectivity of microplastic detection in the presence of ten different potential coexisting contaminants (organic pollutants (1 mg/mL): PFOSA, glyphosate, and thiram; inorganic ions (1mg/mL): chromium, phosphate, and nitrite; inorganic colloids and bio-organisms: clay (TDS 18.06), algae (OD 0.4), and bacteria (OD 0.6); aromatic compound (1mg/mL): bisphenol A) commonly found in real samples, with corresponding Raman intensities at 1066 cm^{-1}. Error bars represent the standard deviations of triplicate measurements.

Figure S10.

Electric field intensity distributions of AgNPs with 2 nm (a) and 10 nm (b) gaps in the vertical plane (x–z), showing the confinement of the localized electric field between the gaps of two adjacent nanoparticles.

Supplementary 1

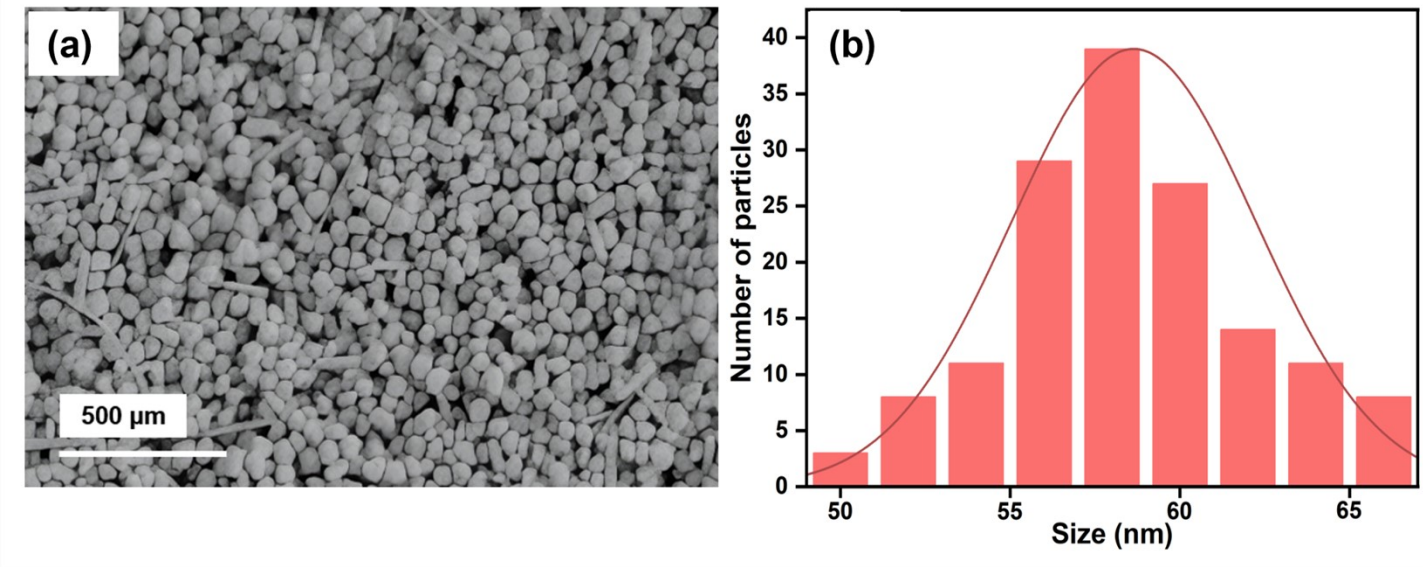

Fig. S1. Scanning electron microscopy image of AgNPs decorated on the filter paper (AgNPs@Filter paper). (b) Histogram size distribution for ~150 random AgNPs across various SEM images with an average size distribution of ~57 ± 5 nm.

Supplementary 2

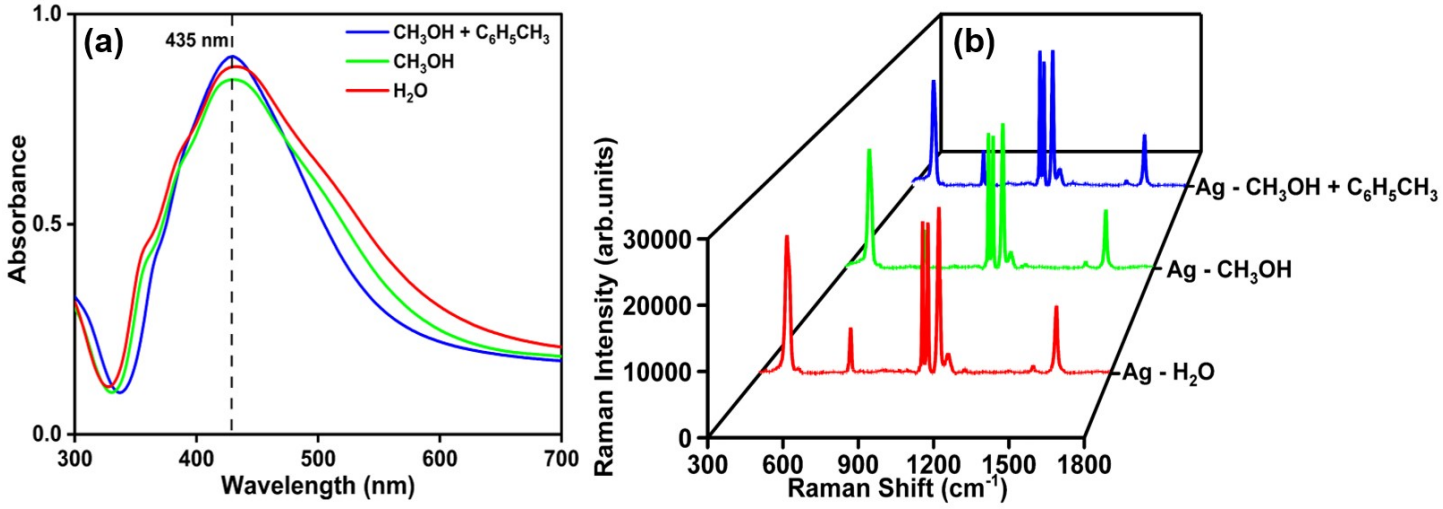

Fig. S2. (a) UV-vis spectra of Ag colloids dispersed in various solvents: deionized (DI) water, methanol, and a methanol-toluene mixture, (b) SERS spectra of 1mM thiophenol adsorbed on Ag colloids dispersed in the solvents: DI water, methanol, and methanol-toluene mixture.

Supplementary 3

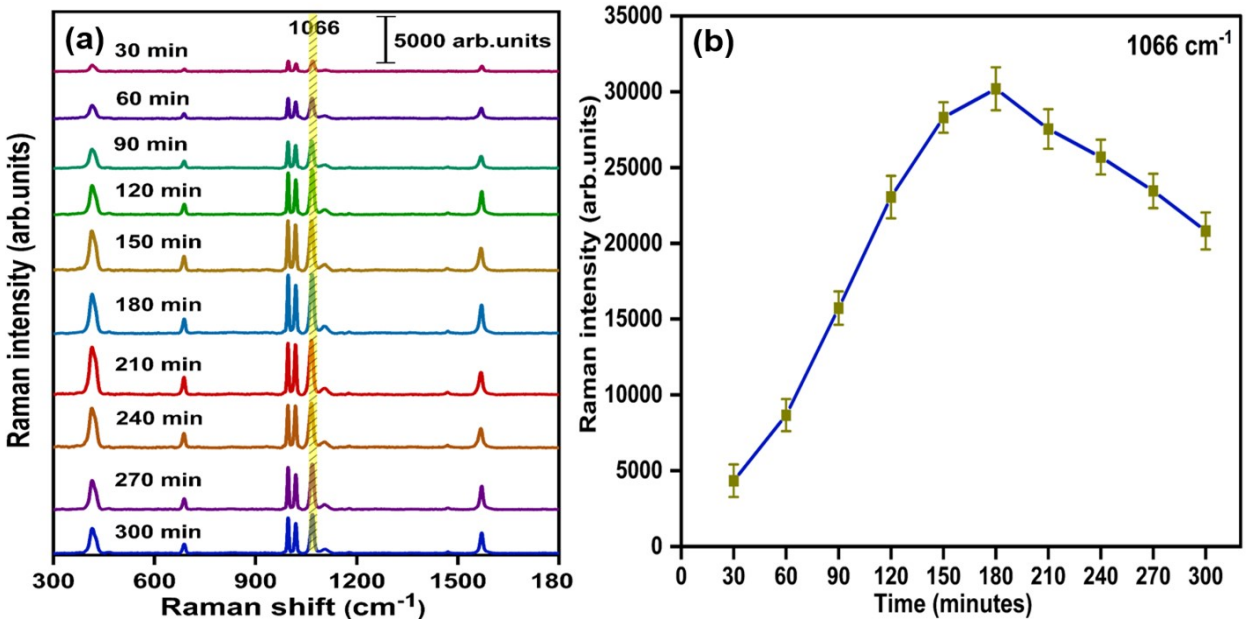

Fig. S3. (a) SERS spectra of 1 mM thiophenol adsorbed on AgNPs@Filter paper substrates, demonstrating the evaporation time from 30 min to 300 min. (b) Corresponding SERS signal at 1066 cm^{-1}.

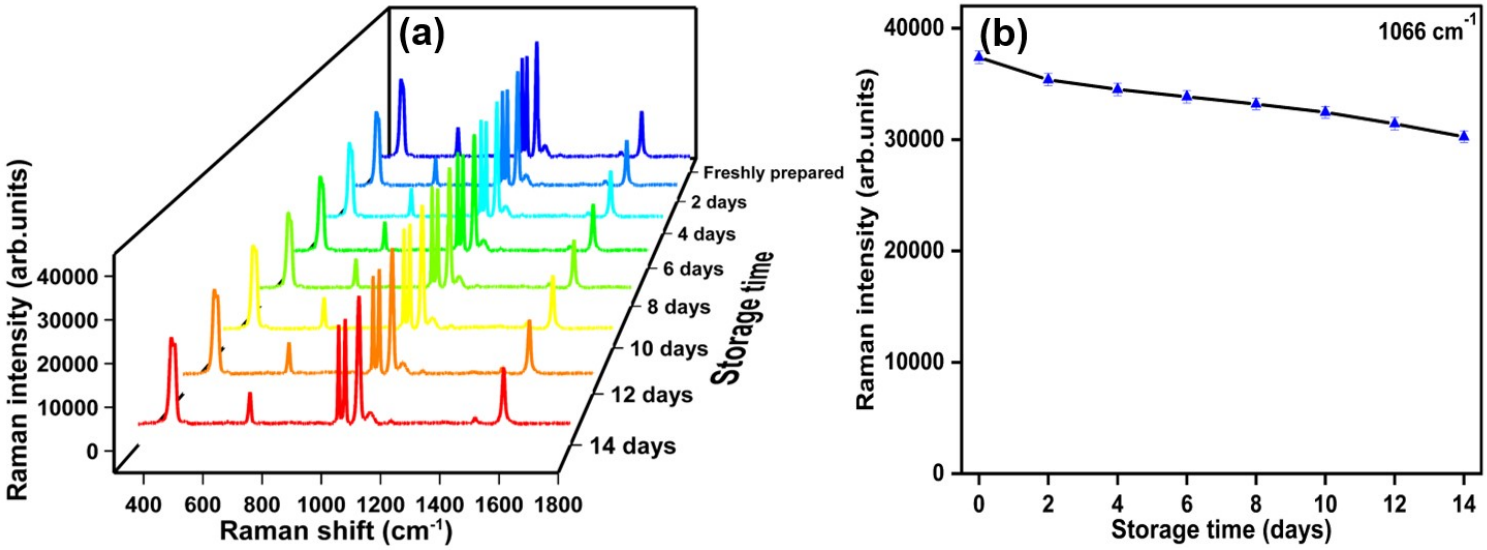

Supplementary 4

Fig. S4. (a) SERS spectra of 1 mM thiophenol adsorbed on AgNPs@Filter paper substrates, demonstrating long-term stability over 14 days. The substrates were sealed and stored at 3 ºC. (b) Corresponding SERS signal at 1066 cm^{-1}.

Supplementary 5

Table. S1. Peak assignments of thiophenol, rhodamine 6G, and malachite green.

Thiophenol - Raman shift (cm^{-1})	**Assignment**
415	υ(C-S) C-S stretching
690	υ(C-C) Ring breathing
1000	υ(C-C) Ring breathing
1020	δ(C-H) C-H in-plane bending
1066	δ(C-H) C-H in-plane bending
1575	υ(C-C) C-C stretching (in phenyl ring)

υ - Stretching vibration

δ - In-plane bending

Rhodamine 6G - Raman shift (cm^{-1})	**Assignment**
610	υ(C-C-C) C-C-C Ring in-plane bending
770	γ(C-H) C-H Out-of-plane bending
1180	δ(C-H) C-H In-plane bending
1307	υ(C-C) Aromatic C-C stretching
1358	υ(C-C) C-C stretching
1509	υ(C-C) Aromatic C-C stretching
1651	υ(C=C) C=C stretching

υ - Stretching vibration

δ - In-plane bending

γ - Out-plane bending

Malachite green - Raman shift (cm^{-1})	**Assignment**
435	δ(ring) Ring deformation
526	δ(C-C-N) C-C-N bending
793	γ(C-H) C-H Out-of-plane bending
920	υ(C-N) C-N stretching
1171	δ(C-H) C-H In-plane bending
1220	δ(C-H) C-H bending
1298	υ(C-N) C-N stretching
1390	υ(N-Ph) N-phenyl stretching
1587	υ(C-C) C-C Ring stretching
1615	υ(C-C) C-C Ring stretching

υ - Stretching vibration

δ - In-plane bending

γ - Out-plane bending

Supplementary 6

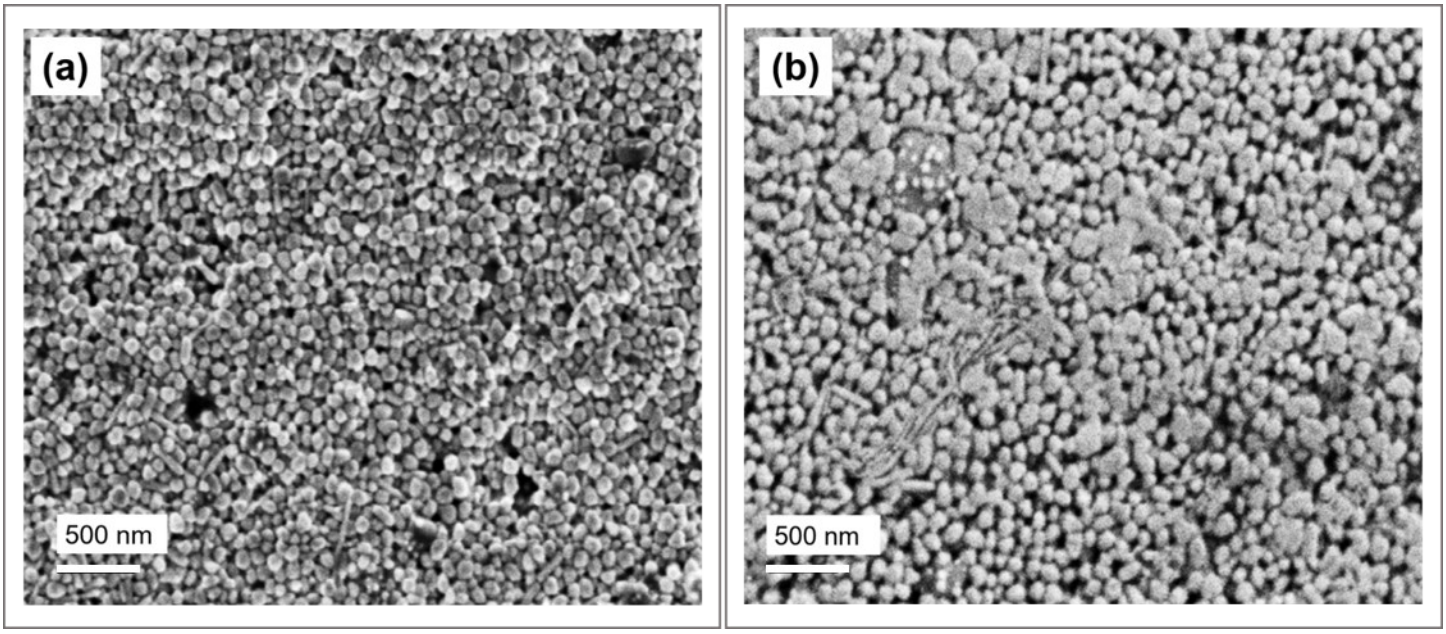

Fig. S5. (a) and (b) Scanning electron microscopic images of AgNPs@Filter paper incubated with concentrations of 0.1 mg/mL and 1 mg/mL of PS microplastic.

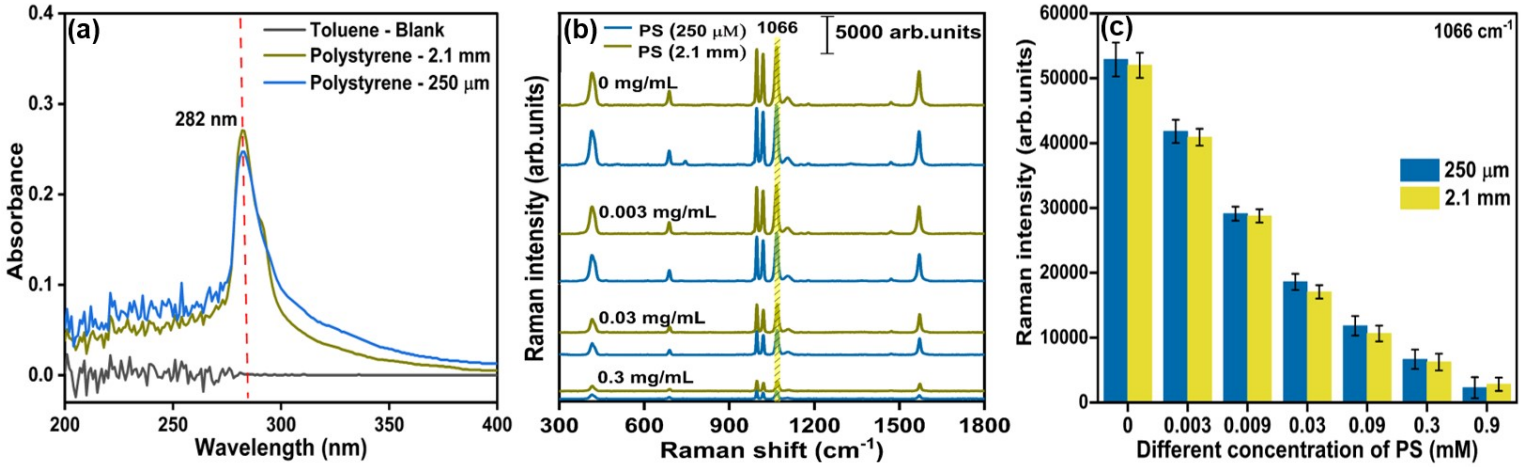

Supplementary 7

Fig. S6. (a) UV-vis spectra of toluene and PS microplastics of varying sizes (250 µm and 2.1 mm) at a concentration of 1 mg/mL dispersed in toluene, (b) SERS spectra of PS (250 µm and 2.1 mm) at different concentrations (0 - 0.3 mg/mL) analyzed on AgNPs@Filter paper substrate using 1 mM thiophenol, (c) corresponding bar graph at 1066 cm^{-1}.

Supplementary 8

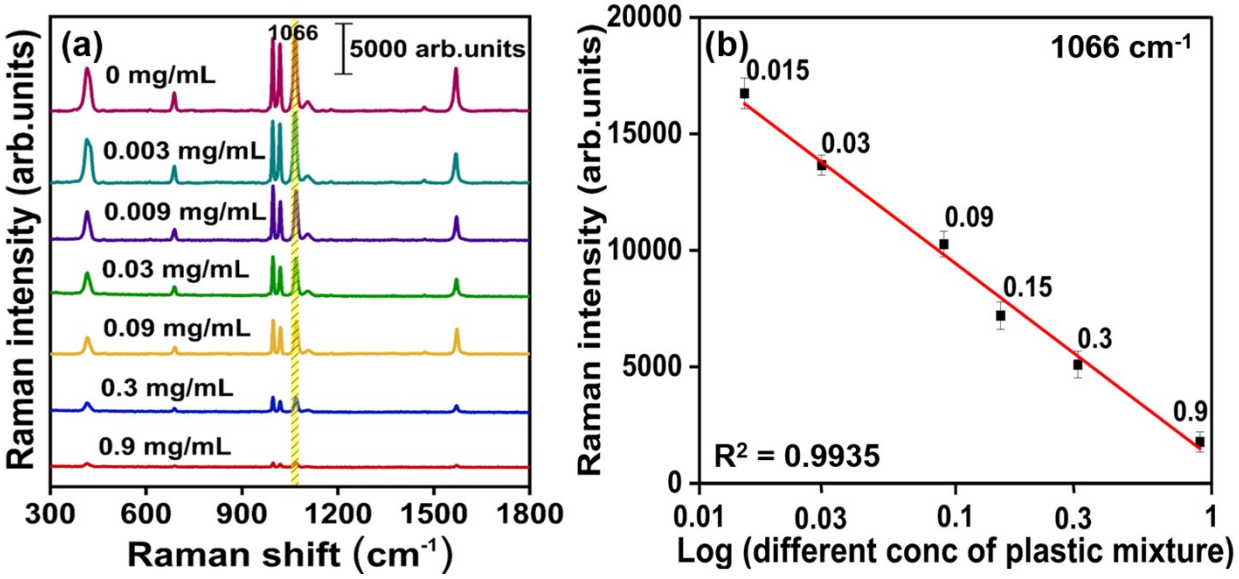

Fig. S7. (a) SERS spectra of various concentrations (0 - 0.9 mg/mL) of microplastic mixtures (PS, PP, and PVC) in equal ratios incubated on an AgNPs@Filter paper substrate were analyzed using 1 mM thiophenol, (b) corresponding linear plot at 1066 cm^{-1}.

Supplementary 9

Table. S2. Water quality parameters for DI, saltwater (salt dissolved in water), and lake water.

Water quality parameters (unit)	DI water	Saltwater	Lake water
pH	8.86	6.94	7.04
Conductivity (µS/cm)	7.35	57,758	1,276.3
Resistivity (Ω cm)	1,36,176	17.31	783.51
Density (g/cm^3)	1.00	1.03	1.00
Salinity (PSU)	0.00	38.51	0.62
ORP (Oxidation reduction potential) (mV)	137.1	125.9	105.5
RDO (Rugged dissolved oxygen) concentration (mg/L)	7.57	6.58	7.94
TDS (Total dissolved solids)	0.00	36.99	0.80

Supplementary 10

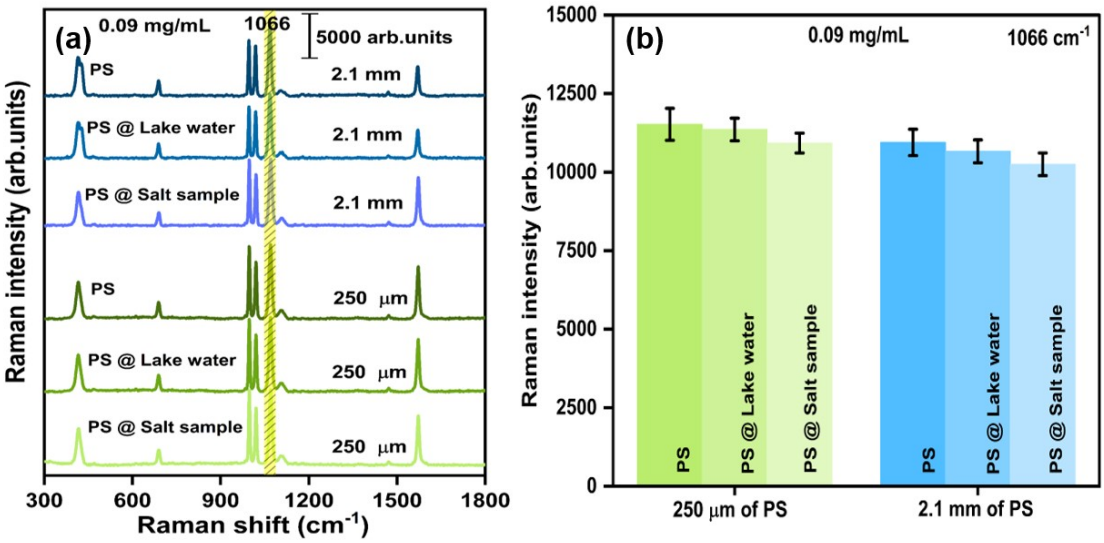

Fig. S8. (a) SERS spectra of 0.09 mg/mL PS microplastics (250 µm and 2.1 mm) spiked in lake water and salt samples, incubated on an AgNPs@Filter paper substrate, and analyzed using 1 mM thiophenol, (b) corresponding bar graph at 1066 cm^{-1}.

Supplementary 11

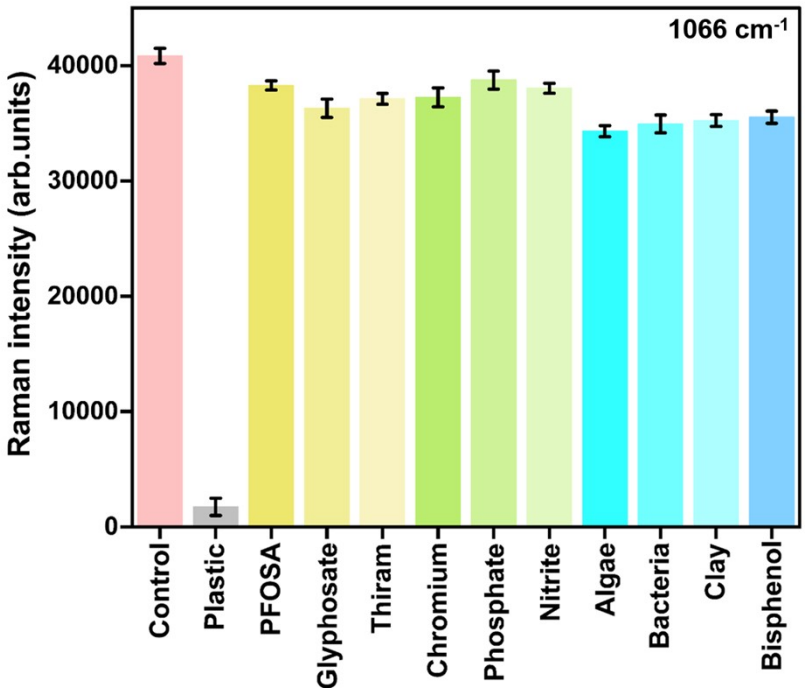

Fig. S9. Bar diagram illustrating the selectivity of microplastic detection in the presence of ten different potential coexisting contaminants (organic pollutants (1 mg/mL): PFOSA, glyphosate, and thiram; inorganic ions (1 mg/mL): chromium, phosphate, and nitrite; inorganic colloids and bio-organisms: clay (TDS 18.06), algae (OD 0.4), and bacteria (OD 0.6); aromatic compound (1 mg/mL): bisphenol A) commonly found in real samples, with corresponding Raman intensities at 1066 cm^{-1}. Error bars represent the standard deviations of triplicate measurements.

Plastic – Polypropylene (PP)

PFOSA – Perfluorooctane sulfonamide

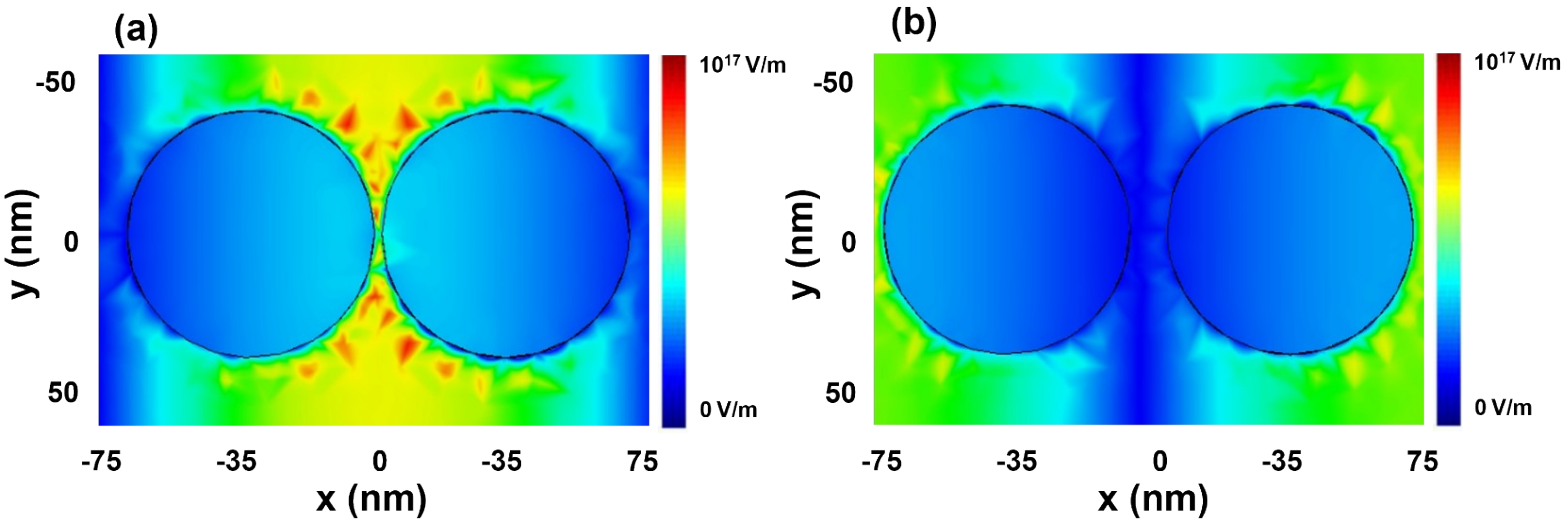

Supplementary 12

Fig. S10. Electric field intensity distributions of AgNPs with 2 nm (a) and 10 nm (b) gaps in the vertical plane (x–z), showing the confinement of the localized electric field between the gaps of two adjacent nanoparticles.